ARMY RESEARCH LABORATORY

Design and Testing of the ARL Squeeze 4 Helical Flux Compression Generator

by Peter Bartkowski and Paul Berning

ARL-TR-6477 June 2013

NOTICES

Disclaimers

The findings in this report are not to be construed as an official Department of the Army position unless so designated by other authorized documents.

Citation of manufacturer's or trade names does not constitute an official endorsement or approval of the use thereof.

Destroy this report when it is no longer needed. Do not return it to the originator.

Army Research Laboratory
Aberdeen Proving Ground, MD 21005-5066

ARL-TR-6477 **June 2013**

Design and Testing of the ARL Squeeze 4 Helical Flux Compression Generator

Peter Bartkowski and Paul Berning
Weapons and Materials Research Directorate, ARL

REPORT DOCUMENTATION PAGE	Form Approved OMB No. 0704-0188

1. REPORT DATE *(DD-MM-YYYY)*	2. REPORT TYPE	3. DATES COVERED (From - To)
June 2013	Final	14 January 2013

4. TITLE AND SUBTITLE
Design and Testing of the ARL Squeeze 4 Helical Flux Compression Generator

5a. CONTRACT NUMBER

5b. GRANT NUMBER

5c. PROGRAM ELEMENT NUMBER

6. AUTHOR(S)
Peter Bartkowski and Paul Berning

5d. PROJECT NUMBER

5e. TASK NUMBER

5f. WORK UNIT NUMBER

7. PERFORMING ORGANIZATION NAME(S) AND ADDRESS(ES)
U.S. Army Research Laboratory
ATTN: RDRL-WMP-E
Aberdeen Proving Ground, MD 21005-5066

8. PERFORMING ORGANIZATION REPORT NUMBER
ARL-TR-6477

9. SPONSORING/MONITORING AGENCY NAME(S) AND ADDRESS(ES)

10. SPONSOR/MONITOR'S ACRONYM(S)

11. SPONSOR/MONITOR'S REPORT NUMBER(S)

12. DISTRIBUTION/AVAILABILITY STATEMENT
Approved for public release; distribution is unlimited.

13. SUPPLEMENTARY NOTES

14. ABSTRACT
The U.S. Army Research Laboratory (ARL) has designed, built, and tested the performance of a helical flux compression generator. The generator design uses an aluminum variable pitch coil machined from a solid tube. The armature is also machined from aluminum and filled with a Comp-B explosive fill. Tests were conducted to map the performance of the generator at several different energy levels. Tests were also performed to investigate variations in the design, such as internal insulation, armature velocity, and load impedance.

15. SUBJECT TERMS
helical magnetic flux compression magnetocumulative generator

16. SECURITY CLASSIFICATION OF:			17. LIMITATION OF ABSTRACT	18. NUMBER OF PAGES	19a. NAME OF RESPONSIBLE PERSON
a. REPORT	b. ABSTRACT	c. THIS PAGE			Peter Bartkowski
Unclassified	Unclassified	Unclassified	UU	18	19b. TELEPHONE NUMBER (*Include area code*) 410-278-0210

Standard Form 298 (Rev. 8/98)
Prescribed by ANSI Std. Z39.18

Contents

List of Figures

List of Tables

1. Introduction

Available onboard energy on current Army vehicle platforms is very limited. The fielding of many pulse power devices is being hampered by the lack of available power on Army vehicle platforms. Smaller pulsed power sources will ease the fielding of such devices. One device that has increased power density for pulsed power applications is the flux compression generator. The device is able to convert stored chemical energy in the form of explosives into a pulsed electrical current. The energy density of modern explosive formulations is orders of magnitude higher than that of more conventional capacitive energy stores. Although these small devices can produce electrical currents in excess of 1 MA they do have severe limitations. One, the device requires a small seed current to start the flux compression process. Two, they are a onetime use device, as it uses a destructive explosive charge to power itself. Three, they are best suited to drive devices with low-electrical impedances.

This report details the design, construction, and testing of a helical flux compression generator. This generator is designed as a stepping stone for the creation of other working devices for specific applications. The intent is to baseline this device's performance and use that data to scale the device to meet future applications. Many different designs exist for flux compression devices (Fowler et al., 1975).[1] For this application, the helical design has been chosen as it has a very high energy and power density.

2. Magnetic Flux Compression Theory

Conductors that move through a magnetic field or compress a magnetic field perform work. This work increases the energy in the system. This mechanical energy is transferred to the electrical system through the use of the magnetic field. In a magnetic flux compressor (MFC), a conductor is propelled using explosives to compress a magnetic field. The result is an increase in current conducting through that conductor. A typical MFC will use a seed current to generate the initial seed magnetic field to be compressed in a shielded enclosure. Then an explosive charge is detonated, decreasing the volume of the shielded enclosure (figure 1). This decrease in volume increases the strength of the magnetic field. As a result, an electrical load connected to the MFC will see an increase or magnification of the initial seed current. Some MFCs are capable of magnifying the seed current by a factor of several hundred. A relatively small initial seed current can be amplified into a much larger pulsed current.

[1] Fowler, C., Caird, R., Garn, W. *An Introduction to Explosive Magnetic Flux Compression Generators*; LA-5; Los Alamos Scientific Laboratory, 1975.

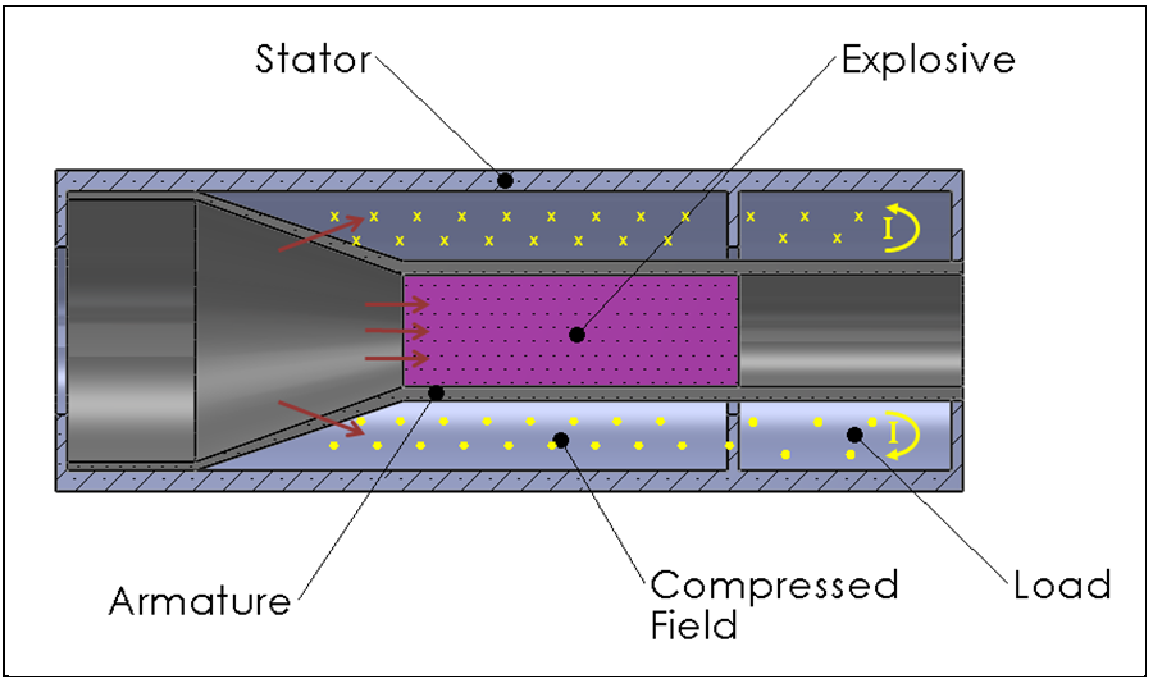

Figure 1. Cross section of coaxial MFC.

3. Basic Governing Equations

The governing flux compression equations are derived from a conservation of flux (L I). Thus, for a loss−less system, the following equation applies:

$$L_0 I_0 = L_1 I_1, \tag{1}$$

or we can predict the peak output current:

$$I_f = \frac{L_0 I_0}{L_f}, \tag{2}$$

where

I = initial seed current

L_0 = initial total system inductance

L_f = final system inductance (load inductance)

In practice, flux losses do occur during the compression due to several factors, such as ohmic heating, flux trapping, arcing, etc. Traditionally, a figure of merit (β) is introduced to account for flux losses during operation. It has a range of 0–1, where a value of 1 indicates a loss−less system. With the addition of β, equation 1 becomes

$$\left(\frac{I_f}{I_0}\right) = \left(\frac{L_0}{L_f}\right)^{\beta}. \quad (3)$$

We can now rearrange to form the following equation to predict peak output current:

$$I_f = I_0 \left(\frac{L_o}{L_f}\right)^{\beta}. \quad (4)$$

The value of the figure of merit gives a good idea of how efficiently the flux compressor is operating. Typical experimental values range from 0.6 to 0.85. As you can see by equation 4, large peak output currents requires either a large initial seed current or a large ratio of initial to final inductances.

4. Design of the Squeeze 4

Coaxial flux compressors typically have good system efficiencies due to the large cross-sectional areas for the current to flow, resulting in low-heating rates and temperatures. However, the coaxial design is relatively inefficient at producing high-initial inductances in compact devices. A helical design was chosen instead to produce a large initial system inductance to help limit the necessary initial seed current. The program goal is to generate a peak current of 2-MA current into a 160-nH load. Figure 2 below shows a cross-sectional view of the Squeeze 4 design.

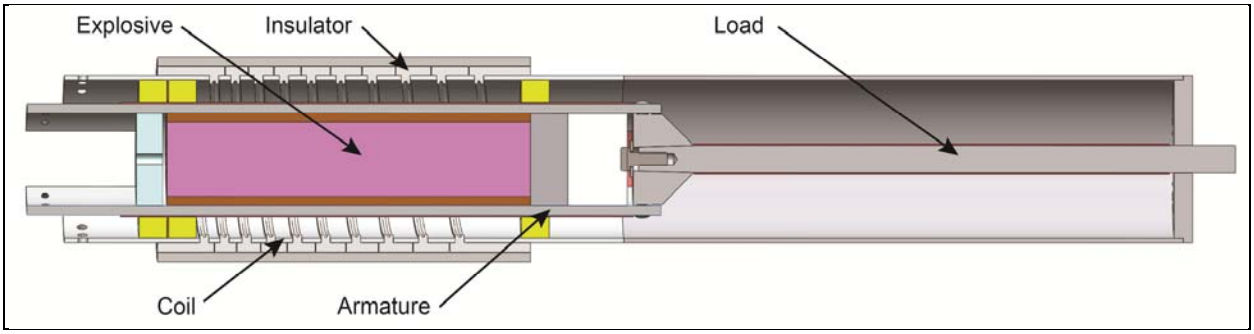

Figure 2. Cross-sectional view of Squeeze 4 design.

One problem helical MFC devices have is handling the large peak currents. In our case, the last winding will be required to handle up to 2 MA of current. Conversely, the first winding will only need to carry the seed current of 100–200 kA. Therefore, a variable pitch coil was chosen that changes the cross-sectional width along the device axis, starting small and getting larger as the current builds in the device. The stator coil was machined from a seamless 6063-T6 aluminum tube (4.5-in outer diameter [OD] and 4.25-in inner diameter [ID]) on a four-axis mill. The coil was designed to have nine turns over an 8-in axial length.

The armature was also machined from a 6061-T6511 seamless aluminum tube (3.0-in OD and 2.5-in ID). This yields an armature expansion ratio of 1.42 and an initial and final wall thickness of 6.4 and 4.5 mm, respectively. An oven was used to shrink polyvinyl chloride (PVC) heat-shrink tubing on the outside of the armature, providing electrical insulation. The PVC thickness after shrinking was ~1 mm thick.

The explosive charge was comprised of a paper-reinforced phenolic cylinder filled with Comp-B explosive fill. The phenolic cylinder was 9.75-in long with a 2.5-in OD and 2.0-in ID. The Comp-B explosive charge filled the interior volume at a 2.0-in diameter, which yields a charge weight of 0.86 kg using a nominal density of 1.72 g/cm^3. Based on a Gurney energy of 4.47 MJ/kg for Comp-B (AMCP, 1972),[2] the armature expansion velocity is calculated using formula 5 to be 2.18 mm/μs:

$$V_c = \sqrt{\frac{2G}{1/2 + M_c/M_e}}, \tag{5}$$

where

G = explosive gurney energy

M_c = mass per unit length of cylinder (includes phenolic)

M_e = mass per unit length of explosive

The armature expansion angle is simply calculated using formula 6 to be 15.2°, using a detonation velocity of 8.0 mm/μs for Comp-B:

$$\theta = \tan^{-1}\left(\frac{V_c}{V_D}\right), \tag{6}$$

where

V_c = cylinder velocity

V_D = detonation velocity

A slotted, 1-mm-thick brass disc was used to crowbar the seed current. The crowbar is necessary to trap the flux within the device and prevent damage to the seed capacitor bank. The slot prevented the formation of eddy currents in the brass disc. The faces of the brass disc were insulated to prevent premature voltage breakdown.

Coil insulation was provided using two techniques. Test 3 used a 1/2-in-thick overwrap of fiberglass tape, which was vacuum wrapped and backfilled with polyester resin. Foam rubber was placed between coil windings (figure 3a). All other subsequent experiments used a custom rapid-prototyped insulator that fitted on the outside and in between coil windings. A ribbed

[2]Pamphlet AMCP 706-180. *Engineering Design Handbook, Principles of Explosive Behavior*, U.S. Army Materiel Command, April, 1972.

protrusion into the coil interior provided additional protection against coil-to-coil surface arcing (figure 3b). Two different protrusion lengths of 0.10 and 0.15 in into the coil cavity were investigated.

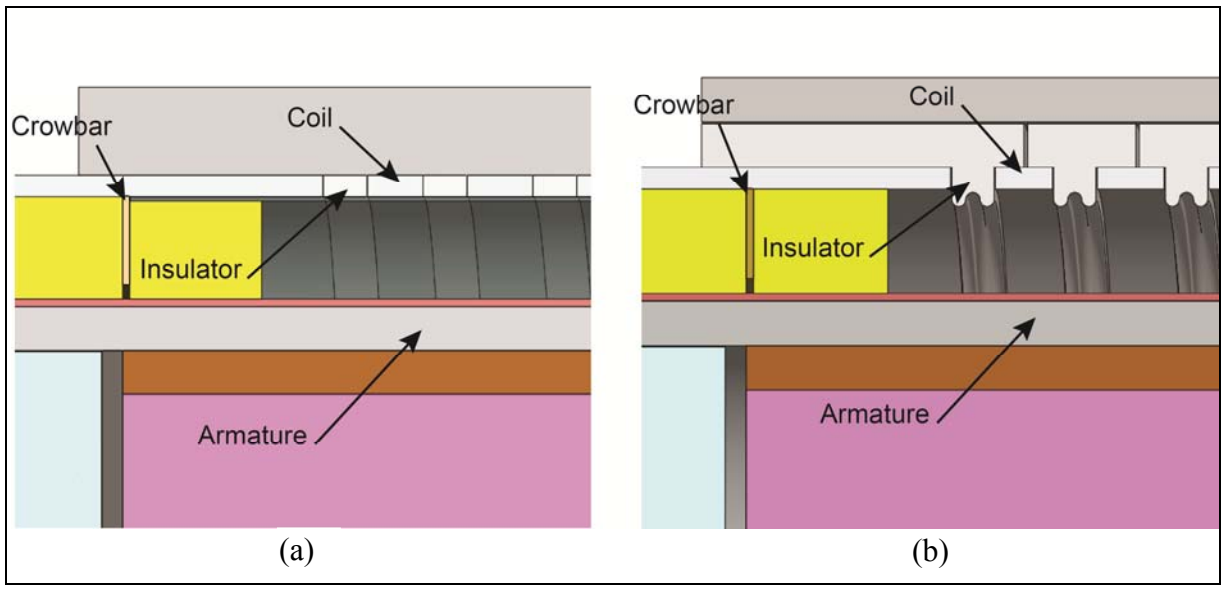

Figure 3. Closeup cross-sectional views of the two coil insulation techniques.

To provide support and alignment to the coil and insulator, a 1/4-in-thick fiberglass tube was slipped over the coil insulator. This also added mass to reduce the velocity of the coil after impact from the armature, increasing pressure and forcing the armature insulation to break down. This creates a sliding arc along the coil helix as the armature makes contact.

Centering the armature inside the coil was accomplished with three machined polyurethane (4 lb/ft^3 Lastafoam)[3] foam rings.

A steel cylinder was placed on the end of the explosive cylinder to act as an anvil, forcing all of the explosive energy at burnout outward into the armature expansion. A 3-mm-thick disc of Primasheet explosive was placed on the initiation end of the explosive charge as a booster. A detonator holder machined from polycarbonate was placed on top of the booster to center the detonator along the device axis.

Notches were machined into the ends of the coil tube and armature tube to aid in the placement of the explosive charge, booster, and detonator.

For these experiments, a benchtop load was used to dissipate the energy from the flux compression device. The load was designed as a coaxial extension of the flux compression device. The tube coaxial output feed of the coil was extended with an aluminum cap placed on the end. The cap acts as the electrical connection between the tube and the 3/4-in diameter load

[3] Lastafoam is a trademark of General Plastics Manufacturing Company.

rod. All experiments used aluminum rods for the load except for the last, which used a stainless steel rod to increase the load resistance. A tapered transition piece connected the load to the end of the armature. This design easily accommodates changes in inductance and resistance by changing the length of the tube and load rod.

Seed current to the device was supplied by a 535-μF high-voltage capacitor bank. Copper stripline conductors connected the capacitor bank to the initiating end of the stator coil and armature. Seed current was changed by varying the charge voltage up to 20 kV. After charging the capacitor bank, a spark gap switch was used to initiate the seed current. After the spark gap was triggered, a timer was used to delay the detonator initiation until the seed current reached peak magnetic field strength.

5. Experimental Data

All data were collected on an Agilent DSO6000 series digital oscilloscope. The data consisted of timing signals for the switch and detonator initiation and current derivative (dI/dt) signals from Rogowski current monitoring cables. Two current monitors were used: one on the capacitor bank to measure the seed current, the other inside the load to measure load current. After the test, the dI/dt signals are digitally integrated to yield the current versus time profiles.

In all, seven experiments were conducted using this flux compressor design. A summary of those tests is given in table 1 below.

Table 1. Summary of experimental tests.

Test No.	Charge Voltage (kV)	Peak Seed Current (kA)	Peak Output Current (kA)	Current Mag. Factor	Figure of Merit (β)	Notes
3	10	123	801	6.51	0.69	Fiberglass overwrap insulator
4	10	117	714	6.10	0.66	Longer coil insulator protrusion
5	20	220	1041	4.73	0.56	Longer coil insulator protrusion
6	6	70	414	5.91	0.63	Longer coil insulator protrusion
7	10	112	818	7.30	0.71	Shorter coil insulator protrusion
8	10	114	875	7.68	0.72	Shorter coil insulator protrusion, faster armature
9	10	121	714	5.90	0.66	Shorter coil insulator protrusion, SS load rod

As seen in the table, a charge voltage of 10 kV was chosen as the baseline for testing. Excursions were made to 20 and 6 kV to investigate the linearity of system response to seed current. Other variations included using a fiberglass overwrap on the coil as an insulator, shortening the insulator protrusions into the flux compression volume, a thinner armature wall thickness to

increase armature expansion velocity, and using a stainless steel load rod to increase load resistance.

The main evaluation criterion was the figure of merit (**β**), with higher values indicating more efficient device performance.

Three different techniques were explored to insulate the coil. During the compression process, voltages of 50–100 kV are not uncommon between the coil and armature. The voltage between neighboring coil windings can also be substantial, typically 5–20 kV. To prevent premature high-voltage breakdown between the coil and armature, PVC heat-shrink tubing was applied to the armature. After shrinkage, the PVC insulation had a nominal thickness of 1 mm. Coil-to-coil insulation was provided by two different techniques. Test 3 used a foam rubber between the windings. All other tests used a custom rapid prototyped insulator that had a protrusion into the interior of the coil to prevent coil-to-coil surface arcing. Two different lengths of protrusion were tested. Tests 4, 5, and 6 had a protrusion of 0.15 in, whereas tests 7, 8, and 9 used a shorter length of 0.10 in. The theory being that the longer protrusions created larger volumes of incompressible space, where flux was not recovered, lowering system efficiency. A comparison of the output currents from the various insulators in tests 3, 4, and 7 are shown in figure 4. As can be seen, the test with the longest protrusions (test 4) yielded the lowest peak current. The test with the foam between the coil winding (no protrusion, test 3) and the test with the shorter insulator protrusion (test 7) yielded similar higher peak currents.

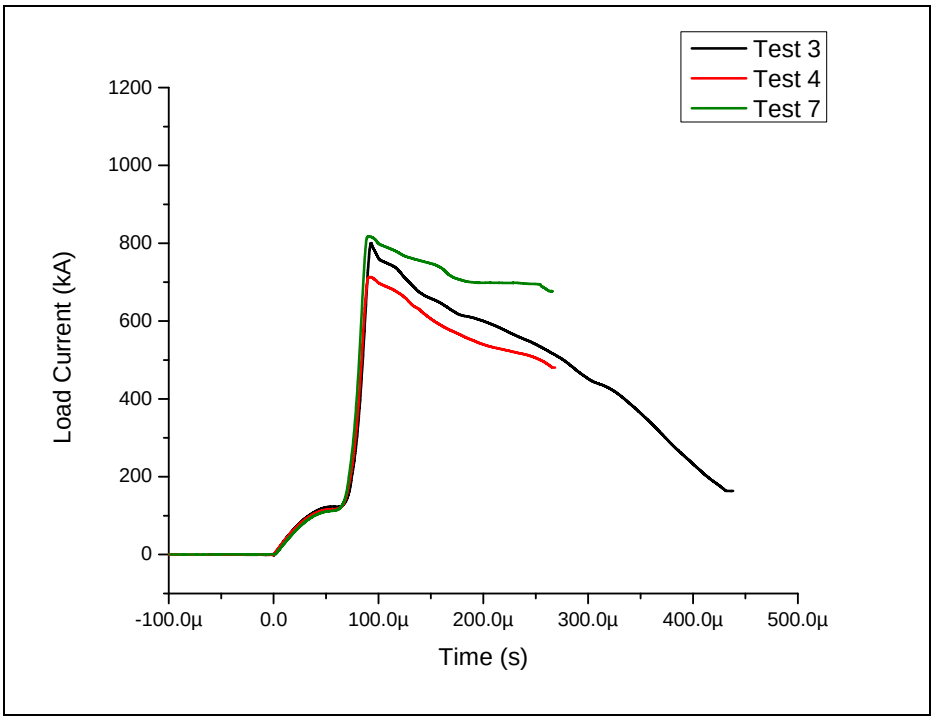

Figure 4. Comparison of output currents with different coil insulators.

Tests were also conducted to investigate the linearity of the device output to variations in seed current. Seed current was changed by varying the initial charge voltage on the capacitor bank. A comparison of three tests (4, 5, and 6), where the charge voltage was changed, can be seen in figure 5. All three tests were conducted with the longer protruding coil insulator. Charge voltages of 6, 10, and 20 kV produced seed currents of 70, 117, and 220 kA, respectively. Peak output currents for the three tests were 414, 714, and 10441 kA, which yielded current magnification ratios of 5.91, 6.10, and 4.73, respectively. The lower magnification ratio from test 5 indicates some nonlinearity. This is most likely due to high temperatures being reached in the coil conductors due to ohmic heating.

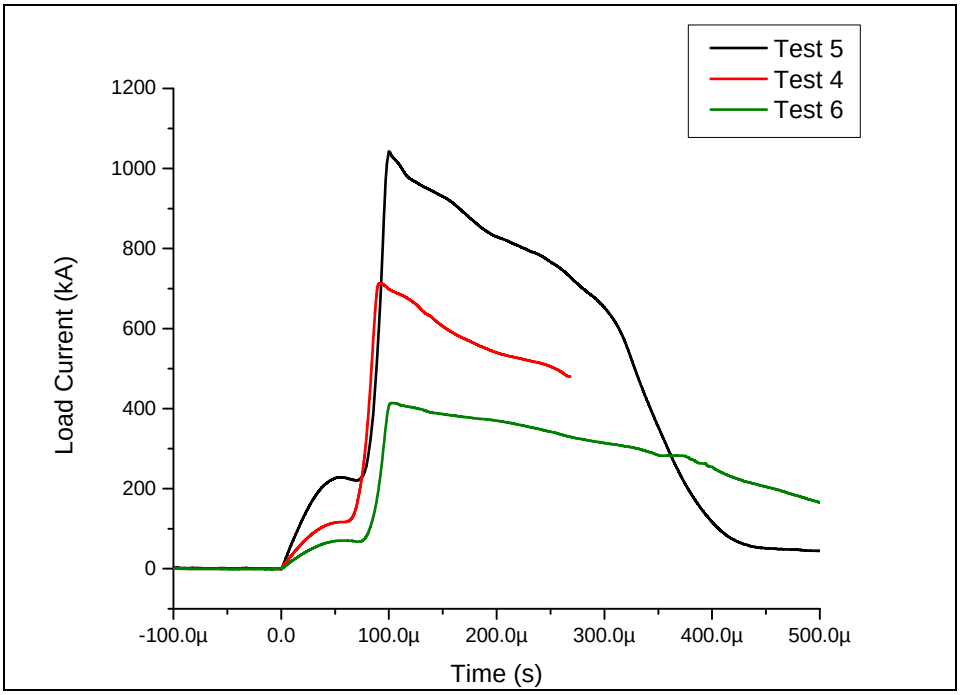

Figure 5. Comparison of output currents with initial charge voltages of 20, 10, and 6 kV.

Two other excursions were taken to determine the effect of a faster armature velocity and having a higher impedance load. In theory, a faster armature velocity will impart more energy to the system, increasing the output current. The faster armature velocity was achieved by machining the armature to a thinner wall thickness of 0.16 in instead of the standard 0.25 in. Also, to further increase velocity, a larger diameter Comp-B explosive charge was used, increasing the explosive energy. To fit a larger diameter charge into the same ID armature, a thinner wall (0.125 in versus 0.25 in) phenolic tube was used. The armature expansion velocity due to these changes was calculated to be 2.78 mm/µs instead of the 2.18 mm/µs in all other tests. As can be seen in figure 6, the peak output current of the faster armature velocity (test 8) was slightly higher than the standard armature (test 7). Interestingly, the numerical simulations of simple coaxial flux compression devices suggested a larger increase in output current than the 7% experimentally seen.

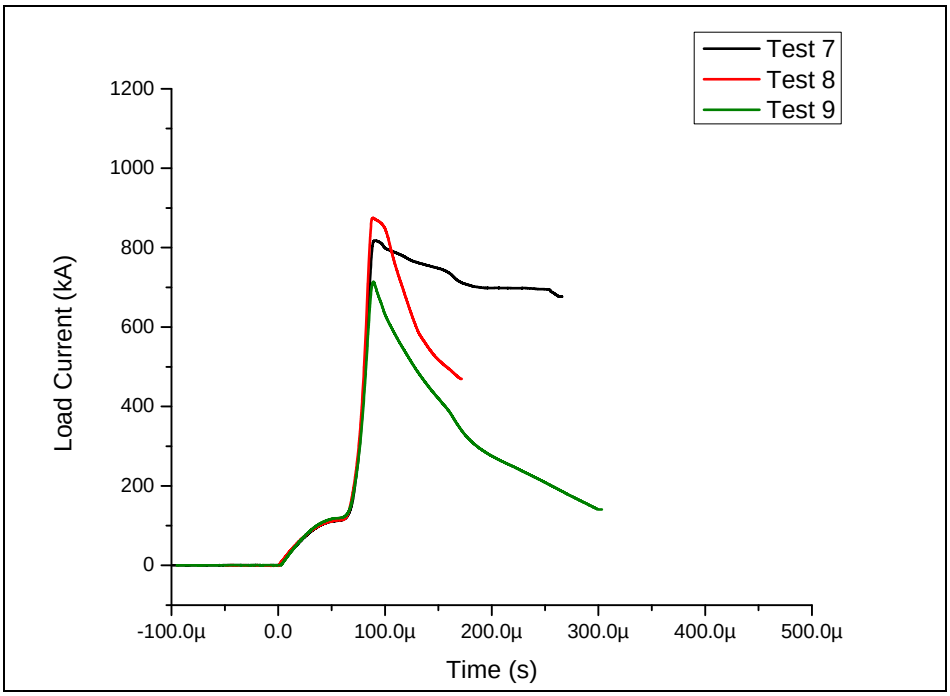

Figure 6. Comparison of output currents with faster armature and high-impedance load.

A higher impedance load will lower output current levels and cause the current to decay faster. To determine the effects of using a higher resistance load, the aluminum load rod was replaced with a stainless steel one. By keeping the geometry the same, the inductance remains constant. The stainless, having a much higher resistivity, only increases the resistance of the load. From the decay of the output current after the peak, the resistance of the aluminum and stainless steel loads were determined to be ~0.35 ± 0.10 mΩ and 1.4 mΩ, respectively. As can be seen in figure 6, the output current using the higher resistance stainless steel load (test 9) is lower in peak current and decays much faster than the aluminum load (test 7).

6. Conclusions

A series of seven flux compression experiments were conducted using a static, benchtop load. Variations were made in the design and seeding of the flux compression device to investigate the changes in output current. Several coil insulation techniques were investigated, as well as the effect of changing input seed current. In other experiments, the armature velocity and load resistance were increased.

All of the coil insulation techniques seem adequate at the initial 10-kV capacitor charge voltage. There were no indications in the output current waveforms that premature voltage breakdown occurred. In theory, the rapid prototyped protruding insulator should have a higher coil-to-coil surface arc potential than the foam winding insulation. Preventing coil-to-coil surface arcing

becomes more important at higher operating voltages. The tests using the shorter protruding insulation had higher system efficiencies. In practice, the shortest necessary protrusion should be used to maximize system performance.

The effect of seed current was noticeable at the 20-kV capacitor initial charge voltage. The figure of merit for that test was significantly lower than the 6-kV and 10-kV charge voltages, which exhibited nearly the same efficiency. This is a sign of nonlinear ohmic heating effects. The higher level of current heats the conductors, lowering the conductivity of the material. This effectively chokes off the current, reducing the peak current level. There are two options to reduce this effect: increasing the width of the conductor or decreasing the resistivity. A new device can be designed that has a wider conductor width. This will lower the current density by increasing the conductor cross section. As the ohmic heating rate is a function of the square of current density, the heating rate will be reduced. Switching to a copper coil will reduce the initial material resistance by ~50%. This will also reduce the heating rate, which should produce higher system output currents.

The effect of increasing armature velocity by 28% only increased peak output current by 7%. We expected a larger increase in peak output current. This lack of sensitivity to armature velocity is interesting and warrants future study.

The effects of increasing load resistance were consistent with theory. The resulting peak output current was lower and the decay rate of the current after burnout (peak current) was much faster. This is expected from an increase in load resistance.

Oddly, the output current profiles from the faster armature and higher impedance tests show similarities. The faster armature profile decay immediately after peak current indicates a similar load resistance to all the other aluminum loads for ~10 μs. After that, the resistance suddenly increases, creating a much faster decay rate, similar to the stainless steel load test. This observation, combined with the lower than expected peak current in the faster armature test, may indicate that the armature was failing during the experiment. Armature failures are typically due to rapid metal fatigue creating axial fracturing at large expansion ratios. This can be controlled to some degree by increasing armature wall thickness and also through annealing of the armatures to increase ductility (Neuber, 2005).[4] All of the armatures in these tests were made from extruded 6061-T6511 aluminum tubing. No additional heat treating or annealing was performed.

Although the Squeeze 4 device design failed to produce the 2-MA output current, the results of this test series have indicated areas for future work. In particular, more work needs to be done at higher seed currents. This is where nonlinear effects become dominant and significantly lower system efficiencies. Alternate coil materials, such as copper, may help reduce the nonlinear effects. The design and function of the armature is also another important area to investigate, particularly at high-expansion ratios. The unexpected large increase in resistance during the faster armature velocity experiment (test 8), may indicate possible armature failing.

[4]Neuber, A. A Explosively Driven Pulsed Power, Springer, 2005.

NO. OF COPIES	ORGANIZATION
1 (PDF)	DEFENSE TECHNICAL INFORMATION CTR DTIC OCA 8725 JOHN J KINGMAN RD STE 0944 FORT BELVOIR VA 22060-6218
1 (PDF)	DIRECTOR US ARMY RESEARCH LAB RDRL CIO LL
1 (PDF)	GOVT PRINTG OFC A MALHOTRA
5 (PDF)	US ARMY TACOM J WHITE L FRANKS D TEMPLETON M LAWSON J HITCHCOCK
2 (PDF)	PM ABCT J ROWE E BARSHAW
4 (PDF)	NATL GROUND INTLLGNC CTR D EPPERLY T SHAVER T WATERBURY D DOBROWOLSKI
1 (PDF)	PM MRAP J PEREZ (JPO)
1 (PDF)	DARPA/DSO L CHRISTODOULOU
1 (PDF)	PM BFVS D SPENCER
1 (PDF)	NSWC CARDEROCK DIV R PETERSON
1 (PDF)	SANDIA NATL LAB E STRACK
1 (PDF)	US ARMY SMDC L ALTGILBERS
1 (PDF)	LOS ALAMOS NATL LAB D REISMAN

NO. OF COPIES	ORGANIZATION
2 (PDF)	BAE SYSTEMS LANDS & ARMAMENTS R APPLETON J PERONA
2 (PDF)	GDLS R NICOL M KAUTZER
1 (PDF)	US ATEC E SANDERSON
	ABERDEEN PROVING GROUND
24 (PDF)	DIR USARL RDRL SED P C TIPTON D PORSCHET RDRL WM P BAKER RDRL WMP S SCHOENFELD RDRL WMP A C HUMMER B RINGERS W UHLIG P BERNING A PORWITZKY RDRL WMP B C HOPPEL RDRL WMP D A BARD R DONEY M KEELE D KLEPONIS J RUNYEON D PETTY RDRL WMP E P BARTKOWSKI S BARTUS M BURKINS D HACKBARTH E HORWATH C KRAUTHAUSER P SWOBODA RDRL WMP F N GNIAZDOWSKI

INTENTIONALLY LEFT BLANK.